Optimization of modified volume Fresnel zone plates

Pornsak Srisungsitthisunti* Okan Ersoy†

Xianfan Xu‡

*Purdue University, psrisung@purdue.edu

†Purdue University - Main Campus, ersoy@purdue.edu

‡Birck Nanotechnology Center, School of Materials Engineering, Purdue University, xxu@purdue.edu

Optimization of modified volume Fresnel zone plates

Pornsak Srisungsitthisunti,[1] Okan K. Ersoy,[2,*] and Xianfan Xu[1]

[1]*School of Mechanical Engineering, Birck Nanotechnology Center, Purdue University, West Lafayette, Indiana 47907*
[2]*School of Electrical and Computer Engineering, Birck Nanotechnology Center, Purdue University, West Lafayette, Indiana 47907*
[*]*Corresponding author: psrisung@purdue.edu*

Received May 28, 2009; revised July 30, 2009; accepted August 4, 2009; posted August 4, 2009 (Doc. ID 112072); published September 1, 2009

Modified volume Fresnel zone plates (MVFZPs) fabricated with laser direct writing were optimized for higher diffraction efficiencies. The Fresnel radii in each layer of a volume zone plate were iteratively adjusted by a simulation-based direct search optimization. The results show that optimization is effective but depends strongly on the starting diffraction efficiencies determined by the MVFZP parameters. The simulations indicate that the optimized MVFZP can achieve 93% diffraction efficiency. © 2009 Optical Society of America

OCIS codes: 320.7110, 050.1970, 130.3120, 000.4430.

1. INTRODUCTION

Recently, modified volume Fresnel zone plates (MVFZPs) consisting of several layers of Fresnel zone plates have been developed to improve diffraction efficiency [1]. In our previous works, we demonstrated high-efficiency MVFZPs fabricated inside a fused silica by a femtosecond laser direct writing method [1,2]. The MVFZP replaces the regular Fresnel zones with central rings [1–3] as shown in Fig. 1 ,since it is practically convenient to fabricate and provides relatively high diffraction efficiency. Our fabricated MVFZP achieved a diffraction efficiency as high as 71% compared with 6% by a single-layer FZP with the same laser writing condition [2]. Therefore, the MVFZP approach is highly suitable for laser direct writing or other methods where the induced phase modulation is limited.

In addition, a beam propagation simulation of MVFZPs has been developed to provide comprehensive studies of various designs of MVFZPs [3]. In this paper, the use of the Hankel beam propagation method (Hankel BPM) is extended for efficiency optimization of MVFZPs. This approach is especially useful for optimizing three-dimensional diffractive optical devices. The motivation behind MVFZP optimization was that multiple diffractions occur inside a MVFZP, and it is difficult to directly design such a device under these complex diffractions [2]. However, the original MVFZP design assumed direct diffraction passing through the subsequent FZP layers neglecting all other diffractions and interferences. As a result, higher diffraction efficiency can possibly be achieved by simply changing the positions of the rings such that more light is diffracted toward a focus spot. For a single-layer FZP, this would not be possible because the original Fresnel zones already provide the smallest phase error for focusing such that the beam is constructively interfered at a focal spot. For the case of MVFZP, the phase shift is altered by subsequent layers and the original Fresnel zones in each layer are not necessarily providing the smallest phase error. Therefore, in this work, MVFZP optimization is investigated to further improve the diffraction efficiency.

The rest of the paper is organized as follows. The direct search optimization method suitable for MVFZP simulation is presented in Section 2. Sections 3 and 4 discuss the results of low-NA and high-NA MVFZP optimizations, respectively. Section 5 studies the influence of the MVFZP linewidth on the starting efficiency. The sensitivity to fabrication errors is analyzed in Section 6 to determine the accuracy required for fabrication of optimized MVFZPs. Conclusions are given in Section 7.

2. METHOD

Several algorithms are available for optimization of diffractive optical elements. Input–output optimization algorithms are widely used, including direct binary search, simulated annealing, and iterative discrete on-axis methods [4]. Some are based on the iterative Fourier transform algorithm (IFTA). The well-known IFTA algorithms are Gerchberg–Saxton, Ping-Pong, Ferwerda, and Yang-Gu [4]. For multiobjective optimization, evolutionary-based programming is preferred, such as the genetic algorithm (GA) [4]. Most of these algorithms optimize results iteratively between input and output planes, so they are not directly applicable for three-dimensional structures.

The direct search optimization is the most straightforward method to use in simulation-based optimization [5]. Diffraction by MVFZP is calculated by the Hankel BPM, which utilizes a split-step angular spectrum representation of plane waves. The direct search method is suitable in our problem in which a computer simulation is run repeatedly in order to compute various quantities needed by the optimization algorithm. Furthermore, the resulting simulation output is then postprocessed to arrive at the

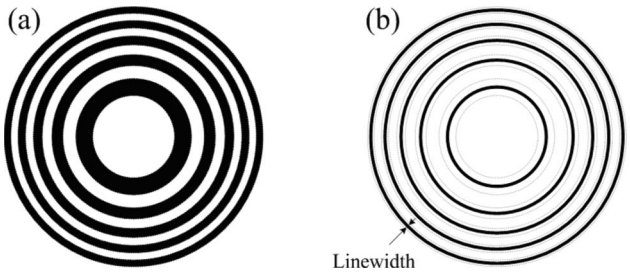

Fig. 1. Comparing the geometry of (a) regular FZP and (b) central-ring FZP. The central-ring FZP has a uniform-linewidth rings located on the middle of the Fresnel zones.

objective value. For example, efficiency calculation cannot be obtained directly from the Hankel BPM, but it is calculated from the overall intensity distribution at the focal plane. The direct search method is sometimes the only option for a complex optimization problem, and usually guarantees convergence [5].

In optimizing central-ring MVFZPs, there are many parameters that affect the simulation results, such as focal length, number of rings (zones), linewidth, and phase modulation. The diffraction efficiency can be increased by adjusting any of these parameters. A brief study of these parameters is available in [3]. It is more meaningful to be able to optimize diffraction efficiency by designing a better MVFZP geometry. In this paper, only the positions of the rings will be adjusted, while other parameters are kept fixed. By moving the positions of the rings, the wavefront is modified and diffracted through multiple layers of MVFZP. Clearly, the rings can be adjusted in either radial or axial direction or both. We decided to adjust the MVFZP rings only in the radial direction to maintain the layered structure for ease of fabrication.

A direct search algorithm is used to optimize the ring positions to provide highest diffraction efficiency. Before optimization, the original locations of the rings follow the Fresnel zone plate equation for central-ring radii given by

$$r_n = \sqrt{\frac{(2n+1)\lambda f}{2} + \left(\frac{(2n+1)\lambda}{4}\right)^2}; \quad n = 1,2,3,\ldots, \quad (1)$$

where f is the focal distance relative to the layer, λ is the wavelength, and n is the ring number. It is expected that by starting with the Fresnel equation, the solution should converge much faster. In each iteration, a ring is randomly selected from any layer of the MVFZP. Then, the radial position is adjusted by a small step in both inward and outward directions. The two cases are treated separately. If the adjusted position improves the diffraction efficiency, the new radius is stored for further evaluation. The position adjustment is terminated as soon as the diffraction efficiency stops increasing. Finally, the new radii of the inward and outward cases are compared, and the one with higher efficiency is saved. This is a completion of one iteration before randomly selecting the next ring. The diagram for one iteration of this algorithm is shown in Fig. 2. Diffraction efficiency is defined by the percentage of light collected within the focal region over the total incident light. We define the focal plane as the plane where the maximum light intensity occurs and the focal spot diameter is equal to $d = 1.22 * \lambda / NA$, given by Rayleigh's criterion.

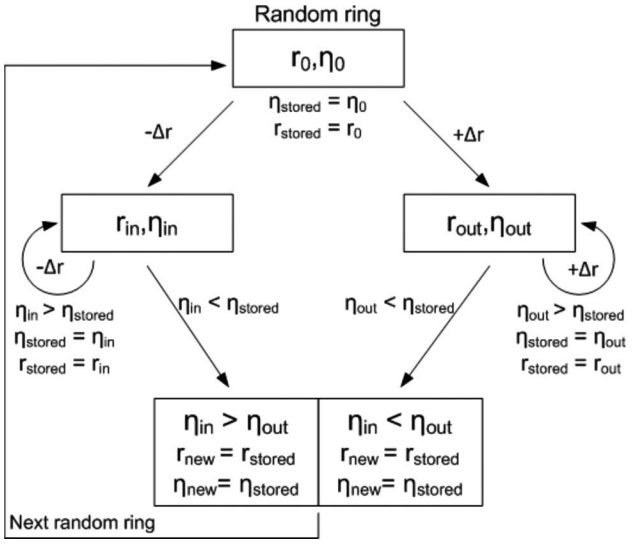

Fig. 2. Direct search algorithm for diffraction efficiency optimization. This is a single iteration including both directions of radius adjustment.

Within one iteration, several recalculations of the Hankel BPM are possibly involved. The direct search algorithm always guarantees convergence, and its accuracy depends on the number of sampling points used. However, a high number of sampling points can lead to a considerably long computational time. As a default, 1500 radial steps and 500 axial steps were used in most MVFZP simulations, which took 21 s per iteration on a 2.0 GHz computer. On the average, using this default resolution, optimization with 1000 iterations was completed in six to eight hours. Using the same algorithm, other quantities can be optimized such as intensity at any location, depth of focus, etc.

3. OPTIMIZATION OF LOW-NA MVFZPS

In this section, optimization of low numerical aperture (NA) MVFZPs is investigated. Previously, the low NA MVFZPs fabricated inside fused silica achieved a diffraction efficiency of 71% [2]. Our optimization simulations were carried out with three different focal lengths: 10 mm (NA=0.037), 20 mm (NA=0.026), and 30 mm (NA =0.021). They had the same parameters for eight layers, ten Fresnel rings (zones) for each layer, 10 μm central-ring width, and phase modulation of 0.23π at each layer. The MVFZPs were designed for the He–Ne laser wavelength, 632.8 nm. These parameters were previously used in femtosecond laser direct writing experiments [1,2]. During optimization, peak intensity and diffraction efficiency were monitored. The peak intensity corresponds to the highest intensity near the focal point. The passing conditions for the storage of each iteration result can be either higher efficiency or higher peak intensity, or both. In this algorithm, the peak intensity was not limited to being located at exactly the design focal length in order to achieve the highest intensity, but it was always very close to it. However, if the exact focal length is critical, the algorithm can be changed to monitor the peak intensity

only at the focal length. The optimization results for the first 1000 iterations are shown in Fig. 3 for peak intensities and their corresponding efficiencies.

In general, all iterations were observed to converge within the first 1000 iterations. The results suggest that the improvements of diffraction efficiency and peak intensity are directly related. The central-ring MVFZPs had different starting diffraction efficiencies of 77.7%, 53.7%, and 31.7% for MVFZPs with focal length of 10 mm, 20 mm and 30 mm, respectively. The uniform linewidth strongly influenced the starting efficiencies of these MVFZPs. The selected linewidth determines how closely the Fresnel zones are approximated by uniform central-ring zones. The 10 μm linewidth was best fit for the 10 mm focal length MVFZP, and a larger linewidth is preferred for a MVFZP with longer focal length. The optimized efficiencies were 92.7%, 71.0%, and 48.9% for MVFZPs with focal lengths of 10 mm, 20 mm and 30 mm, respectively. As such, the efficiency improved by 19.4%, 32.2%, and 54.0% for MVFZPs with focal lengths of 10 mm, 20 mm, and 30 mm, respectively, with the same initial conditions. Therefore, optimization was more effective with MVFZPs with lower starting efficiencies. During optimization, it was found that the MVFZP rings were adjusted only slightly in order to significantly improve diffraction efficiency. For instance, the optimized MVFZP of 20 mm focal length had an average ring position shift of 2.9 μm. Therefore, high efficiency is very sensitive to the positions of the rings. As a related topic, we investigate the effect of position errors on difraction efficiency in Section 5.

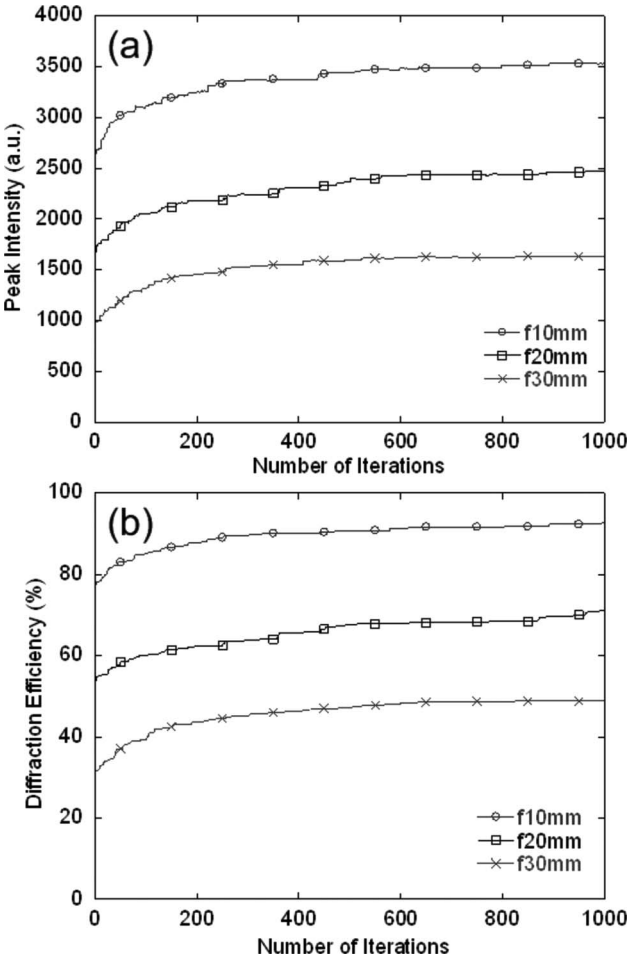

Fig. 3. (a) Peak intensities and (b) their corresponding diffraction efficiencies of low NA MVFZP optimizations during the first 1000 iterations. Three low NA MVFZP were simulated: f =10 mm (NA=0.037), f=20 mm (NA=0.026), and f=30 mm (NA =0.021).

To show the details of how the optimization algorithm changes the output light distribution of a MVFZP, Fig. 4 compares the normal MVFZP output and optimized MVFZP output for the 20 mm MVFZP. Optimization was observed to have slight effects on the FWHM and the depth of focus (DOF) of the beam. The higher-order foci appeared to be suppressed by optimization, especially with the second order. We believe that this suppression is due to the randomness of the rings which breaks the symmetry required for higher-order foci. Suppression of higher-order foci with a modified FZP by using a nonuniform zone-width-to-radius ratio was also reported in [6].

4. OPTIMIZATION OF HIGH-NA MVFZPS

High-NA MVFZPs are significant in high-resolution applications, but they were previously subject to low diffraction efficiencies. To demonstrate the diffraction efficiency improvement of high-NA MVFZPs, we optimized three MVFZPs having focal length of 10 μm (NA=0.82), 20 μm (NA=0.67), and 30 μm (NA=0.58). Other parameters were kept constant as follows: eight layers of zone plates, ten rings, central-ring width of 1 μm, and phase modulation of 0.23π. The MVFZPs were designed for the He–Ne laser wavelength at 632.8 nm. The simulation results are shown in Fig. 5. The simulations showed that the higher-NA MVFZPs typically have lower efficiencies and lower peak intensities. In general, high-NA MVFZPs perform relatively poorly because it is more difficult to diffract light at a larger angle. However, the optimized MVFZP with 10 μm focal length significantly improved its efficiency from 12.1% to 20.1%. The 20 μm MVFZP's efficiency increased from 32.0% to 60.1%, and 30 μm high-NA MVFZP's efficiency increased from 52.3% to

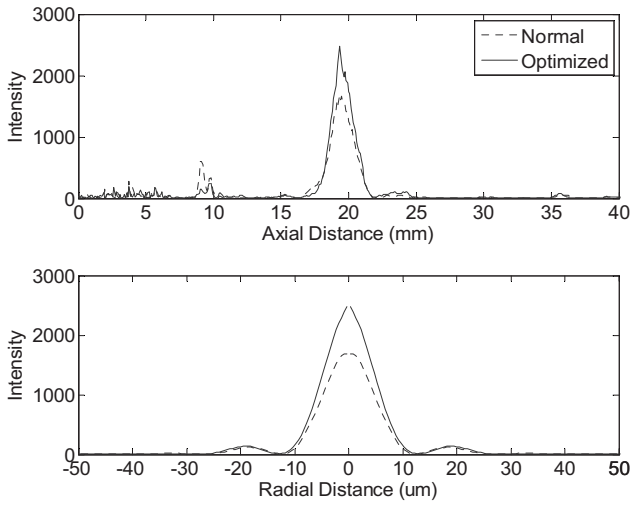

Fig. 4. Optimized result of a low NA MVFZP with a focal length of 20 mm (NA=0.026).

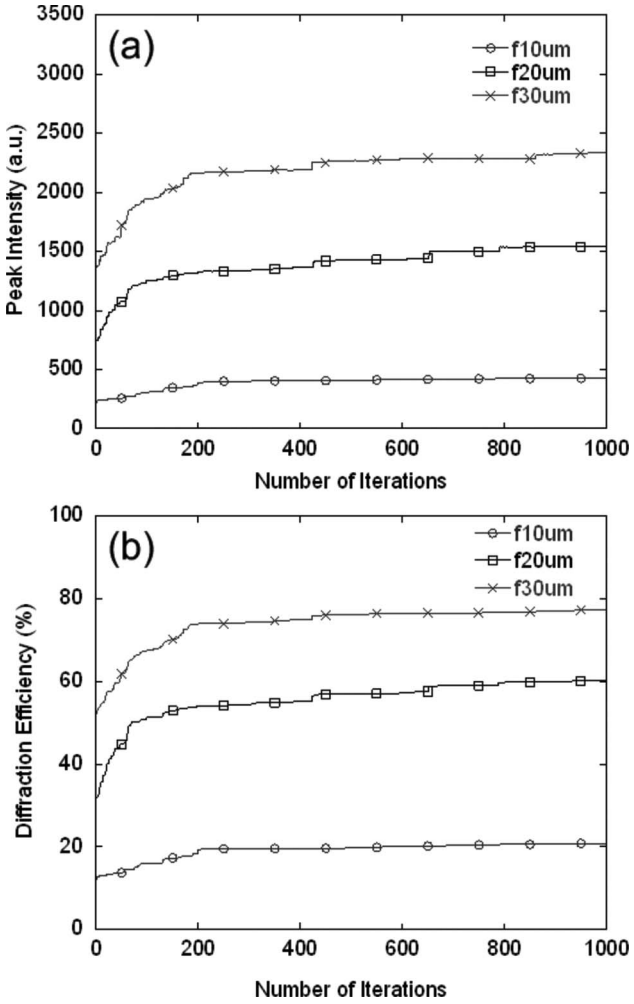

Fig. 5. (a) Peak intensities and (b) their corresponding diffraction efficiencies with high NA MVFZP optimizations during the first 1000 iterations. Three high NA MVFZP were simulated: f =10 μm (NA=0.82), f=20 μm (NA=0.67), and f=30 μm (NA =0.58).

77.3%. These results indicate that optimization is effective in increasing diffraction efficiencies, especially when the starting efficiencies are low. High-NA MVFZPs with initial high efficiencies could not improve much further, whereas the low efficiency MVFZPs could double their efficiencies. In an additional test, the MVFZP with NA =0.92 showed efficiency improvement from 7.2% to 15.6%. Similar to low-NA MVFZP results, the linewidth plays an important role on determining the starting efficiency. A 1 μm linewidth seemed to be best fit for the focal length of 30 μm or larger. The zone width of a regular FZP decreases nonlinearly from center to outer zones, but the average width of the first ten zones for FZPs with 10 μm, 20 μm, and 30 μm focal lengths are 0.56 μm, 0.73 μm, and 0.87 μm, respectively. Hence, it is not surprising that the 1 μm linewidth is more efficient for the MVFZP with 30 μm focal length. Nevertheless, this average linewidth estimation should not be applied to low-NA MVFZPs since the zone width of a regular low-NA FZP decreases much more rapidly. The average width of the first ten zones for regular FZPs with 10 mm, 20 mm, and 30 mm focal lengths are 4.7 μm, 6.7 μm, and 26.0 μm, respectively. The standard deviations of the average zone widths of low-NA FZPs are much higher than those of the high-NA FZPs, and the optimal linewidth cannot be estimated from the average linewidth. For high-NA MVFZP, the rings were finely adjusted and the optimized MVFZP of 20 μm focal length had an average ring position shift of only 0.16 μm.

Figure 6 displays the light distribution for high-NA MVFZPs before and after optimization. Even though the rings are designed for 20 μm focal length, the focus was shifted toward the MVFZP by 4.6 μm. The similar focal shift and higher-order foci suppression were observed in simulation results of near-field zone plates [7]. Our finite-difference time-domain (FDTD) simulations also evidenced a focal shift of the near-field FZP (not shown in this paper). These observations indicate that the Fresnel equation is not very accurate in the near-field region. To accurately design a near-field MVFZP, evanescent waves and/or surface plasmons must be considered. Comparing between the original and the optimized MVFZP, the focal shift during optimization is relatively small. In addition to the focal shift, the higher-order foci of these MVFZPs were suppressed.

5. EFFECT OF LINEWIDTH ON DIFFRACTION EFFICIENCY

In Section 4 the optimizations of MVFZPs were investigated based on the experimental parameters. In this connection, the linewidths for low-NA and high-NA MVFZPs were chosen as 10 μm and 1 μm, respectively. In this section, the influence of linewidth on starting efficiency and optimization is further investigated. Figure 7 compares MVFZPs having the same focal length of 20 mm and various linewidths from 2 μm to 20 μm. For a small linewidth, the optimization is not effective since only a small portion of light is diffracted by the MVFZP no matter how the rings are adjusted. A large linewidth is expected to suffer from low diffraction resulting in a small efficiency increase during optimization. The optimal linewidth provides conditions for effective optimization. In fact, optimization works well when the linewidth is not too far from the optimal range.

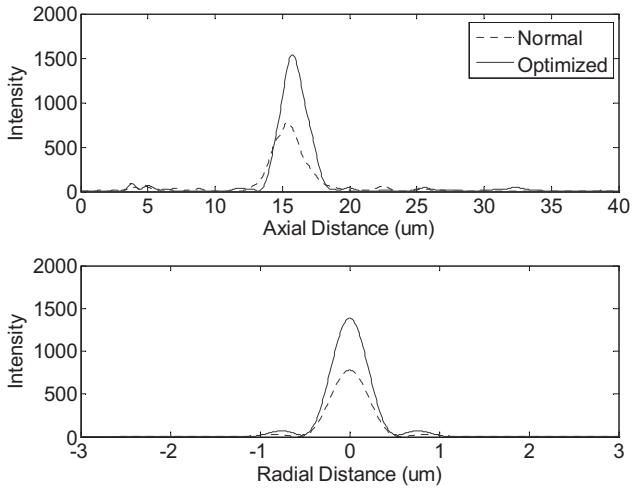

Fig. 6. Optimized result of a high NA MVFZP with a focal length of 20 μm (NA0.67).

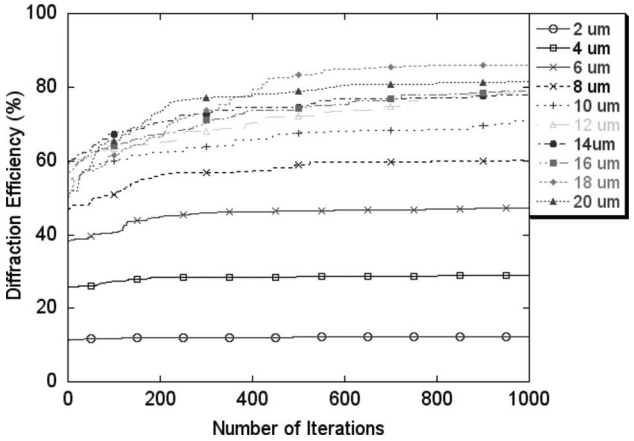

Fig. 7. Optimization of MVFZP having 20 mm focal length with different linewidth ranging from 2 μm to 20 μm.

To estimate the optimal linewidth at different focal lengths, we calculated low-NA MVFZP efficiencies for different combinations of linewidth and focal length before optimization, as shown in Fig. 8. The results indicate a single high-efficiency region concentrated around 10 μm linewidth at 10 mm focal length. This confirms that an optimal linewidth exists and significantly influences optimization at a focal length below 25 mm. Without optimization, the MVFZPs can provide efficiency more than 84% for certain parameters (for example, 4 mm focal length and 6 μm linewidth). However, in practice, a MVFZP is designed at arbitrary focal length and the experimental linewidth is not completely controllable. Therefore, optimization is needed to improve the efficiency and allows more flexible MVFZP design. Similarly, the optimal linewidth was studied for high-NA MVFZP, and the result is shown in Fig. 9. The optimal linewidth is around 0.7 μm for focal length in the range of 10–50 μm.

In addition, two optimizations of different combinations with similar starting efficiencies are compared. The two combinations include 21 mm focal length with 16 μm linewidth and 16 mm focal length with 7 μm linewidth. Both MVFZPs have starting efficiency around 54%, and the optimization results are shown in Fig. 10. The results show different optimization capabilities. The 21 mm focal length showed an efficiency increase to 79%, while the

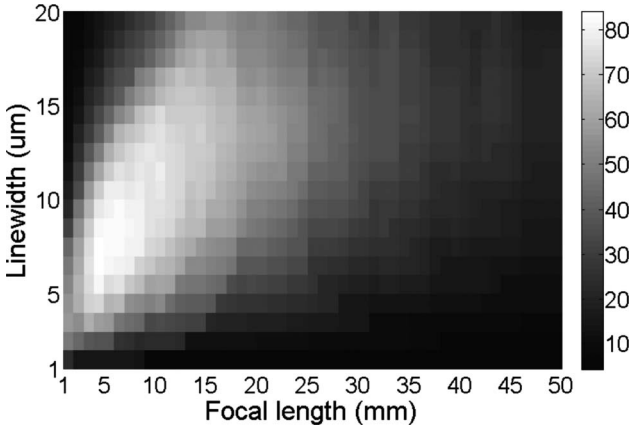

Fig. 8. Diffraction efficiencies before optimization with various focal lengths and linewidths for low NA MVFZP.

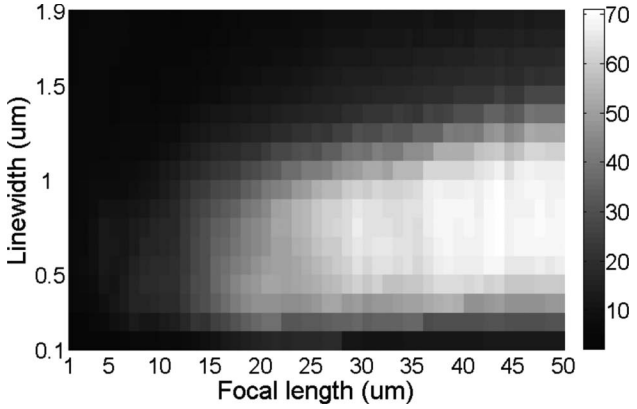

Fig. 9. Diffraction efficiencies before optimization with various focal lengths and linewidths for high NA MVFZP.

16 mm focal length showed an efficiency increase to 63%. This implies that the optimized efficiency is independent of the starting efficiency and is difficult to estimate without optimization.

6. STUDY OF SENSITIVITY TO FABRICATION ERRORS

In practice, there are experimental errors in laser direct writing of MVFZPs due to machine accuracy, fluctuation in laser source, external disruptions, etc. By investigating the effects of fabrication errors, one can understand the error tolerances of the optimized MVFZP designs. The fabrication errors can be generated in axial and radial directions. In sensitivity studies to be reported, the given error was added to the radial or axial position of the optimized MVFZP. Each ring was randomly modified with the given error; then, the modified diffraction efficiency was calculated. We investigated the effects of fabrication errors for low-NA and high-NA MVFZPs separately. Since the introduced errors are random, each result was obtained by averaging over 5–10 trials.

The effects of errors on low-NA and high-NA MVFZPs are shown in Figs. 11 and 12, respectively. For the MVFZP with NA=0.026, the efficiency started to drop

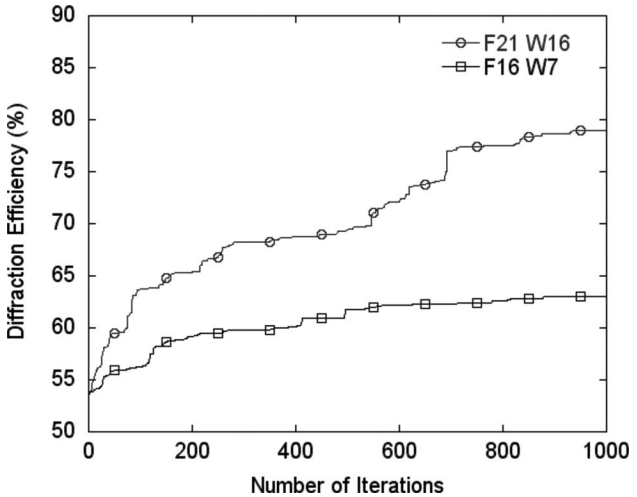

Fig. 10. Optimization of two linewidth and focal length combinations that have similar starting efficiency.

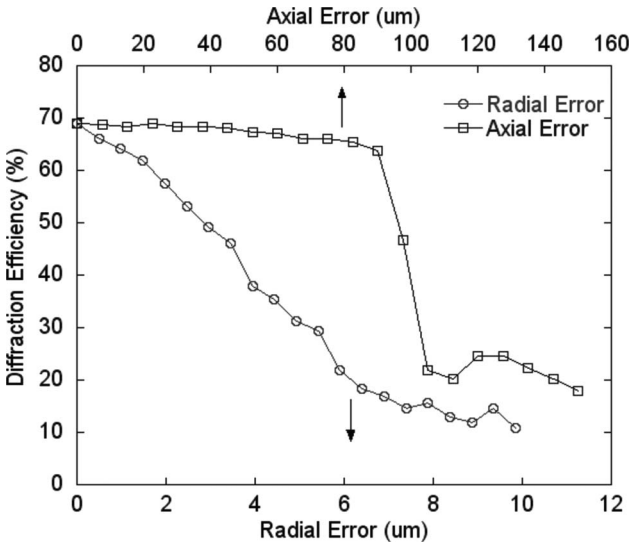

Fig. 11. Fabrication error simulations of low NA MVFZP (NA =0.026).

about 10% when the axial error was greater than 90 μm and the radial error was greater than 1 μm. On the other hand, the MVFZP with NA=0.67 tolerated axial error of only 300 nm and radial error of 100 nm for approximately 10% efficiency decrease. For both cases, the radial error is more critical than the axial error for optimized MVFZPs.

In laser direct writing fabrication, the lateral accuracy depends on the stage accuracy, and the axial accuracy depends on the focal depth of the writing laser. The accuracy of radial position is approximately 1 μm with our air bearing linear stage (Aerotech). This accuracy is sufficient for fabrication of low-NA MVFZPs but not for fabrication of high-NA MVFZPs. The high-NA MVFZP requires piezo stages to achieve submicrometer resolution. The actual axial position is somewhat difficult to specify since the focus spot is elongated inside a transparent material due to spherical aberration [8]. As a result, the elongated focus spot induces additional error in the axial direction.

Finally, the effect of error in phase modulation was analyzed, and the result is shown in Fig. 13. The MVFZPs

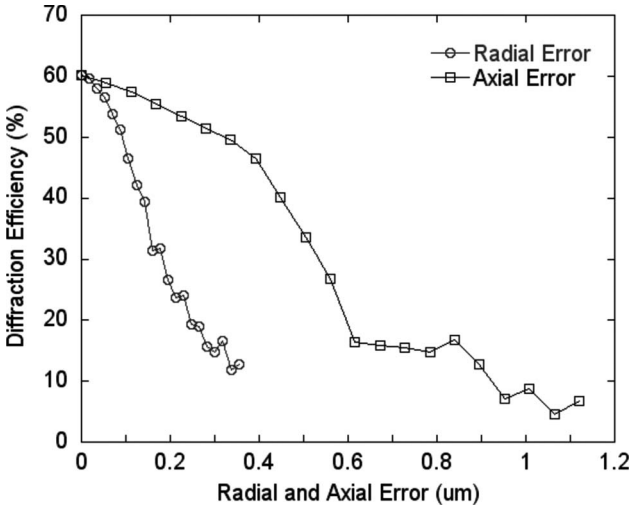

Fig. 12. Fabrication error simulations of high NA MVFZP (NA =0.67).

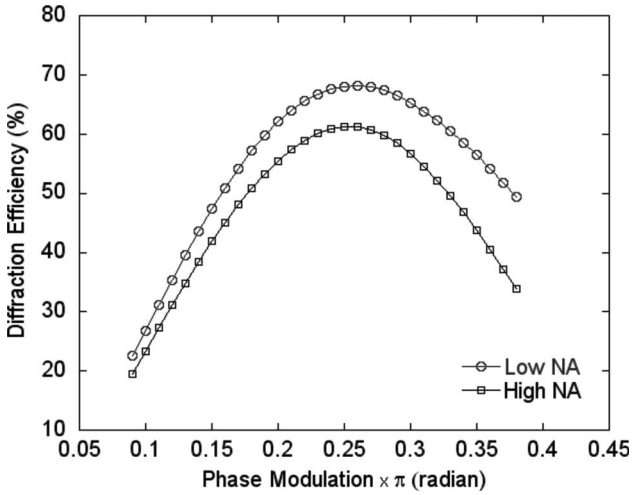

Fig. 13. Phase error simulations of low and high NA MVFZPs.

used in this study were optimized at 0.23π phase modulation, but the highest efficiency occurred around 0.26π. This is unexpected but implies that the optimized condition also performs well for a slightly higher phase modulation. The efficiency curves show unsymmetrical shape, and the negative phase error has larger efficiency reduction compared to positive phase error. In either case, the phase error of 0.05π results in efficiency drop within 10%. Phase error is directly related to the thickness of the FZP layer. Therefore, the phase error of 0.05π is equivalent to about 15 μm of thickness error (at $\lambda=633$ nm and $\Delta n=0.001$), which is relatively large. In other words, the phase error is much less sensitive compared with the axial positional error.

7. CONCLUSIONS

The direct search optimization of MVFZPs was investigated. The approach has shown considerable improvement in diffraction efficiency over original MVFZP design. The algorithm used in our direct search optimization is straightforward, and all simulations converged relatively fast. The efficiency increase strongly depended on the starting efficiency, which is controlled by the MVFZP parameters, especially linewidth. Thus, it is important to select a linewidth close to the optimal linewidth to have a high starting efficiency and effective optimization. In practice, for femtosecond laser direct writing fabrication, many parameters are not completely flexible, such as index change, laser induced cross section, etc. Under these limited conditions, the direct search optimization becomes truly useful. It is able to optimize for the most efficient design under given constraints.

The optimized low-NA MVFZP was shown to achieve maximum diffraction efficiency of 93%, improved from a diffraction efficiency of 71% for the original design. The high-NA MVFZP efficiencies also improved significantly. Optimized MVFZP was achieved with only slight ring position shifts from the original design with no difference in fabrication time, cost, complications, etc. The gained efficiency is due to change in geometry. The sensitivity studies showed that the optimized low-NA MVFZP is robust against fabrication errors. However, the optimized

high-NA MVFZP requires more accurate fabrication technology, and the allowable error is within 100 nm. In the future, MVFZP will be optimized for smaller focal spots while maintaining high efficiencies. This multiobjective optimization is also possible with a similar approach.

ACKNOWLEDGMENT

The authors gratefully acknowledge the funding provided by the Nanoscale Interdisciplinary Research Teams (NIRT) program of the National Science Foundation (NSF) under contract NIRT-0707817.

REFERENCES

1. P. Srisungsitthisunti, O. K. Ersoy, and X. Xu, "Volume Fresnel zone plates fabricated by femtosecond laser direct writing," Appl. Phys. Lett. **90**, 011104 (2007).
2. P. Srisungsitthisunti, O. K. Ersoy, and X. Xu, "Laser direct writing of volume modified Fresnel zone plates," J. Opt. Soc. Am. B **24**, 2090–2096 (2007).
3. P. Srisungsitthisunti, O. K. Ersoy, and X. Xu, "Beam propagation modeling of modified volume Fresnel zone plates fabricated by femtosecond laser direct writing," J. Opt. Soc. Am. A **26**, 188–194 (2009).
4. B. Kress and P. Meyrueis, *Digital Diffractive Optics: An Introduction to Planar Diffractive Optics and Related Technology* (Wiley, 2000).
5. T. G. Kolda, R. M. Lewis, and V. Torczon, "Optimization by direct search: new perspectives on some classical and modern methods," SIAM Rev. **45**, 385–482 (2004).
6. Q. Cao and J. Jahns, "Modified Fresnel zone plates that produce sharp Gaussian focal spots," J. Opt. Soc. Am. A **20**, 1576–1581 (2003).
7. R. G. Mote, S. F. Yu, B. K. Ng, W. Zhou, and S. P. Lau, "Near-field focusing properties of zone plates in visible regime—New insights," Opt. Express **16**, 9554–9564 (2008).
8. N. Huot, R. Stoian, A. Mermillod-Blondin, C. Mauclair, and E. Audouard, "Analysis of the effects of spherical aberration on ultrafast laser-induced refractive index variation in glass," Opt. Express **15**, 12395–12408 (2007).